Available online at www.sciencedirect.com
SCIENCE DIRECT®
Journal of the Mechanics and Physics of Solids
54 (2006) 1401–1425
JOURNAL OF THE MECHANICS AND PHYSICS OF SOLIDS
www.elsevier.com/locate/jmps

Solutions of inhomogeneity problems with graded shells and application to core–shell nanoparticles and composites

H.L. Duan, Y. Jiao, X. Yi, Z.P. Huang, J. Wang*

LTCS and Department of Mechanics and Engineering Science, Peking University, Beijing 100871, PR China

Received 6 January 2006; accepted 18 January 2006

Abstract

This paper first presents the Eshelby tensors and stress concentration tensors for a spherical inhomogeneity with a graded shell embedded in an alien infinite matrix. The solution is then specialized to inhomogeneous inclusions in finite spherical domains with fixed displacement or traction-free boundary conditions. The Eshelby tensors in the infinite and finite domains and the stress concentration tensors are especially useful for solving many problems in mechanics and materials science. This is demonstrated on two examples. In the first example, the strain distributions in core–shell nanoparticles with eigenstrains induced by lattice mismatches are calculated using the Eshelby tensors in the finite domains. In the second example, the Eshelby and stress concentration tensors in the three-phase configuration are used to formulate the generalized self-consistent prediction of the effective moduli of composites containing spherical particles within the framework of the equivalent inclusion method. The advantage of this micromechanical scheme is that, whilst its predictions are almost identical to the classical generalized self-consistent method and the third-order approximation, the expressions for the effective moduli have simple closed forms.

Keywords: Eshelby tensor; Stress concentration tensor; Finite domain; Core–shell nanoparticle; Effective modulus

*Corresponding author. Tel.: +86 10 6275 7948.
E-mail address: jxwang@pku.edu.cn (J. Wang).

0022-5096/$ - see front matter © 2006 Elsevier Ltd. All rights reserved.
doi:10.1016/j.jmps.2006.01.005

1. Introduction

The synthesis and characterization of particles with core–shell structures have attracted a lot of attention in many areas of science and technology. In materials science and engineering, these particles have been used as reinforcements and toughening in composites. In solid-state physics, core–shell nanoparticles are found to exhibit novel physical effects and properties, such as quantum confinement effect, and novel electronic, magnetic and optical properties (e.g. Zhou et al., 1996; Rockenberger et al., 1998; Brongersma, 2003; Goncharenko, 2004). Core–shell particles can be used as functional devices on their own, besides being a constituent part of a composite medium (e.g. Williamson and Zunger, 1999; Lauhon et al., 2002; Abe and Suwa, 2004; Goncharenko, 2004). Many researchers have studied the strain distributions in heterogeneous electronic structures of fine scale, e.g. quantum dot structures (Gosling and Willis, 1995; Freund and Johnson, 2001; He et al., 2004) and shown that the strain affects the optical properties of these structures by modifying the energies and wave functions of the confined carriers. For core–shell nanoparticles, as pointed out by Little et al. (2001), and Perez-Conde and Bhattacharjee (2003), the misfit strain, the surface stress and the applied external pressure all modify the strain fields in them, which in turn affect the electronic structures, and hence their physical properties.

Core–shell structures also widely exist in conventional particle-reinforced composites and nanocomposites due to complicated interactions between the particle surface and the matrix (e.g. Theocaris, 1987; Tzika et al., 2000) and the need for good bond between the reinforcement and the matrix. The elastic properties of the interphase can be uniform or variable through its thickness (Ostoja-Starzewski et al., 1996). The inhomogeneity problems with graded interphases have attracted a lot of attention (e.g. Lutz and Zimmerman, 1996; Wang and Jasiuk, 1998). However, almost all the existing works on inclusion/inhomogeneity problems with graded (inhomogeneous) interphases are concerned with the solutions of stress fields under special loading conditions or with the predictions of effective elastic moduli. It is noted that Ding and Weng (1998), and Weng (2003) have predicted the effective bulk moduli of composites containing spherical particles and graded matrices using a three-phase model containing a graded interphase.

The Eshelby formalism (Eshelby, 1957, 1959) for an inclusion/inhomogeneity is one of the cornerstones in the solutions of many problems in materials science, solid-state physics and mechanics of composites. The classical Eshelby formalism is for an inclusion/inhomogeneity without an interphase in an infinite matrix. In this paper, we shall give the solution of the Eshelby formalism for a spherical particle with a graded interphase embedded in an infinite medium. The Eshelby tensors in the whole region when an eigenstrain is prescribed in the particle and the stress concentration tensors under remote loading will be presented. When the stiffness of the infinite medium is set to be infinite or zero, the Eshelby tensors in a finite domain with a fixed displacement or traction-free boundary condition are given. The application of the Eshelby formalism in the finite and infinite domains is demonstrated on two examples, namely, the calculation of the strains in core–shell nanoparticles and the prediction of the effective moduli of particle-reinforced composites.

2. Solution of spherical inhomogeneity with graded interphase

Consider a spherical inhomogeneity with a graded interphase embedded in an infinite elastic matrix, as shown in Fig. 1. The radius of the inhomogeneity and the outer radius of

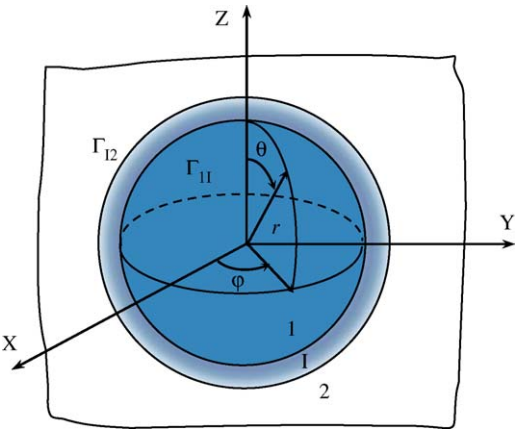

Fig. 1. A spherical inhomogeneity (1) with an interphase (I) in an infinite matrix (2).

the interphase are denoted by a and b, respectively. For brevity, in the following, all length scales are regarded as being normalized by the radius of the inhomogeneity. The interface between the inhomogeneity and interphase is denoted by Γ_{1I} ($r=1$), and the interface between the interphase and matrix is denoted by Γ_{I2} ($r=b/a$). The inhomogeneity and matrix are homogeneous, linearly elastic and isotropic, characterized by the bulk modulus κ_k, the shear modulus μ_k and the Poisson ratio ν_k. Here, and in the following, the subscript and superscript $k=1,I,2$ denote the inhomogeneity, the interphase and the matrix, respectively. For expediency, define modulus ratio $g_{ij}=\mu_i/\mu_j$ ($i,j=1,I,2$). In the spherical coordinate system (r,θ,φ), with the origin coinciding with the centre of the spherical inhomogeneity, the bulk and shear moduli of the interphase are assumed to be power-law functions of r

$$\kappa_I(r)=\kappa_0 r^Q, \quad \mu_I(r)=\mu_0 r^Q, \quad \nu_I=\text{const.}, \tag{1}$$

where κ_0,μ_0 and Q are constants.

Assume that the inhomogeneity is subjected to a uniform eigenstrain $\boldsymbol{\varepsilon}^*$. It is expedient to split the eigenstrain tensor into its dilatational part $\varepsilon_m^*\mathbf{I}^{(2)}$ and deviatoric part $\boldsymbol{\varepsilon}_e^*$, i.e.

$$\boldsymbol{\varepsilon}^*=\varepsilon_m^*\mathbf{I}^{(2)}+\boldsymbol{\varepsilon}_e^*, \tag{2}$$

where $\varepsilon_m^*=(\operatorname{tr}\boldsymbol{\varepsilon}^*)/3$. Thus, the solution under the uniform eigenstrain $\boldsymbol{\varepsilon}^*$ is obtained by the superposition of the solutions under $\varepsilon_m^*\mathbf{I}^{(2)}$ and $\boldsymbol{\varepsilon}_e^*$, respectively. In the following, the solution under $\varepsilon_m^*\mathbf{I}^{(2)}$ will be called a dilatational solution, and that under $\boldsymbol{\varepsilon}_e^*$ a deviatoric solution.

We solve first the *inhomogeneous inclusion* problem with the graded interphase when the only non-zero component of $\boldsymbol{\varepsilon}^*$ is ε_{zz}^*. Obviously, the displacements in the interphase for the dilatational part of ε_{zz}^* have the following form in the spherical coordinate system:

$$u_r^I=\omega_r^I(r), \quad u_\theta^I=0, \quad u_\varphi^I=0. \tag{3}$$

Substituting Eqs. (1) and (3) into the equilibrium equations gives

$$\frac{\mathrm{d}^2\omega_r^I}{\mathrm{d}r^2}+\frac{(2+Q)}{r}\frac{\mathrm{d}\omega_r^I}{\mathrm{d}r}+\left(\frac{2\nu_I Q}{1-\nu_I}-2\right)\frac{\omega_r^I}{r^2}=0. \tag{4}$$

The solution of Eq. (4) is

$$\omega_r^I(r) = F_{zz}^I r^{h_5} + G_{zz}^I r^{h_6},$$
$$h_5, h_6 = -\frac{1}{2}\left[Q + 1 \mp \sqrt{Q^2 + 9 + Q\frac{(2-10\nu_I)}{(1-\nu_I)}}\right], \tag{5}$$

where F_{zz}^I and G_{zz}^I are constants to be determined by the continuity and boundary conditions, and the subscript zz indicates that the solution is for the eigenstrain component ε_{zz}^*.

Now we consider the deviatoric solution for ε_{zz}^*. By analogy with the solutions for homogeneous media, we assume that the displacements for the graded interphase have the following form in the spherical coordinate system:

$$u_r^I(r,\theta) = U_r^I(r)P_2(\cos\theta), \quad u_\theta^I(r,\theta) = U_\theta^I(r)\frac{\mathrm{d}P_2(\cos\theta)}{\mathrm{d}\theta}, \quad u_\varphi^I(r) = 0, \tag{6}$$

where $P_2(\cos\theta)$ is the Legendre polynomial of order two, and $U_r^I(r)$ and $U_\theta^I(r)$ are unknown functions of r. Substituting Eq. (6) along with Eq. (1) into the equilibrium equations gives

$$\begin{aligned}
&[Q+4-2\nu_I(Q+2)]U_r^I + r\frac{\partial U_r^I}{\partial r} - [Q+12-2\nu_I(Q+6)]U_\theta^I \\
&\quad + (Q+2)(1-2\nu_I)r\frac{\partial U_\theta^I}{\partial r} + (1-2\nu_I)r^2\frac{\partial^2 U_\theta^I}{\partial r^2} = 0, \\
&[2\nu_I(Q+4)-5]U_r^I + (Q+2)(1-\nu_I)r\frac{\partial U_r^I}{\partial r} + (1-\nu_I)r^2\frac{\partial^2 U_r^I}{\partial r^2} \\
&\quad + 3[3-2\nu_I(Q+2)]U_\theta^I - 3r\frac{\partial U_\theta^I}{\partial r} = 0.
\end{aligned} \tag{7}$$

To solve Eq. (7), we introduce the operator (Wylie and Barrett, 1982)

$$r^m\frac{\partial^m U}{\partial r^m} = h(h-1)\ldots(h-m+1)U. \tag{8}$$

Substituting Eq. (8) into Eq. (7), while eliminating U_r^I and U_θ^I, gives a characteristic equation in h

$$\begin{aligned}
&(1-\nu_I)h^4 + (2-2\nu_I+2Q-2Q\nu_I)h^3 + (Q^2-Q^2\nu_I+Q \\
&\quad + Q\nu_I + 13\nu_I - 13)h^2 + (3Q^2\nu_I - Q^2 + 17Q\nu_I - 15Q + 14\nu_I - 14)h \\
&\quad + (4Q^2\nu_I + 4Q\nu_I - 4Q - 24\nu_I + 24) = 0.
\end{aligned} \tag{9}$$

Eq. (9) has two sets of roots. The first set contains real roots, and the second contains complex ones. The four real roots h_1, h_2, h_3 and h_4 are

$$\begin{aligned}
h_1 &= -\frac{Q+1}{2} + \frac{\sqrt{R-T}}{2\sqrt{1-\nu_I}}, \quad h_2 = -\frac{Q+1}{2} - \frac{\sqrt{R-T}}{2\sqrt{1-\nu_I}}, \\
h_3 &= -\frac{Q+1}{2} + \frac{\sqrt{R+T}}{2\sqrt{1-\nu_I}}, \quad h_4 = -\frac{Q+1}{2} - \frac{\sqrt{R+T}}{2\sqrt{1-\nu_I}},
\end{aligned} \tag{10}$$

where

$$R = (1 - v_I)(Q^2 + 4Q + 29) - 4Qv_I,$$
$$T = 2\sqrt{(1 - v_I)[-25Q^2 v_I + 44Q - 100(Qv_I + v_I - 1)] + Q^2(3v_I + 1)}. \tag{11}$$

The corresponding displacement fields in the graded interphase are given in Eq. (6) with

$$U_r^I(r) = A_{zz}^I r^{h_1} + B_{zz}^I r^{h_2} + C_{zz}^I r^{h_3} + D_{zz}^I r^{h_4},$$
$$U_\theta^I(r) = \widetilde{A}_{zz}^I r^{h_1} + \widetilde{B}_{zz}^I r^{h_2} + \widetilde{C}_{zz}^I r^{h_3} + \widetilde{D}_{zz}^I r^{h_4}, \tag{12}$$

where $A_{zz}^I, B_{zz}^I, C_{zz}^I, D_{zz}^I, \widetilde{A}_{zz}^I, \widetilde{B}_{zz}^I, \widetilde{C}_{zz}^I$ and $\widetilde{D}_{zz}^I$ are constants to be determined from the continuity and boundary conditions. Substituting Eq. (12) into Eq. (7) gives the corresponding relations between $A_{zz}^I, B_{zz}^I, C_{zz}^I, D_{zz}^I$ and $\widetilde{A}_{zz}^I, \widetilde{B}_{zz}^I, \widetilde{C}_{zz}^I, \widetilde{D}_{zz}^I$

$$\Xi_i = -\widetilde{\Xi}_i \frac{12 - 12v_I + Q(1 - 2v_I) - (1 - 2v_I)[h_i(Q + 1) + h_i^2)]}{(2Qv_I - Q - h_i - 4 + 4v_I)}, \tag{13}$$

where $i = 1, 2, 3, 4$, Ξ_1, Ξ_2, Ξ_3 and Ξ_4 stand for $A_{zz}^I, B_{zz}^I, C_{zz}^I$ and D_{zz}^I, respectively, and $\widetilde{\Xi}_1, \widetilde{\Xi}_2, \widetilde{\Xi}_3$ and $\widetilde{\Xi}_4$ for $\widetilde{A}_{zz}^I, \widetilde{B}_{zz}^I, \widetilde{C}_{zz}^I$ and $\widetilde{D}_{zz}^I$, respectively. The complex roots (two pairs of complex conjugate roots) of Eq. (9) are

$$h_1 = m_1 + \mathrm{i}d_1, \quad h_2 = m_1 - \mathrm{i}d_1, \quad h_3 = m_2 + \mathrm{i}d_2, \quad h_4 = m_2 - \mathrm{i}d_2, \tag{14}$$

where

$$m_1 = m_2 = -\frac{Q + 1}{2}, \quad d_1 = \frac{\sqrt{R + T}}{2\sqrt{1 - v_I}}, \quad d_2 = \frac{\sqrt{R - T}}{2\sqrt{1 - v_I}}. \tag{15}$$

The displacement fields in the graded interphase corresponding to these complex roots are again given by Eq. (6) with

$$\begin{aligned} U_r^I(r) = {} & A_{zz}^I \cos(d_1 \ln r) r^{m_1} + B_{zz}^I \sin(d_1 \ln r) r^{m_1} \\ & + C_{zz}^I \cos(d_2 \ln r) r^{m_2} + D_{zz}^I \sin(d_2 \ln r) r^{m_2}, \\ U_\theta^I(r) = {} & \widetilde{A}_{zz}^I \cos(d_1 \ln r) r^{m_1} + \widetilde{B}_{zz}^I \sin(d_1 \ln r) r^{m_1} \\ & + \widetilde{C}_{zz}^I \cos(d_2 \ln r) r^{m_2} + \widetilde{D}_{zz}^I \sin(d_2 \ln r) r^{m_2}. \end{aligned} \tag{16}$$

Substituting Eq. (16) into Eq. (7) gives the corresponding relations between A_{zz}^I, $B_{zz}^I, C_{zz}^I, D_{zz}^I$ and $\widetilde{A}_{zz}^I, \widetilde{B}_{zz}^I, \widetilde{C}_{zz}^I, \widetilde{D}_{zz}^I$, i.e.

$$A_{zz}^I = \frac{H_A}{X} \tag{17}$$

in which

$$
\begin{aligned}
H_A = {} & \widetilde{A}^I_{zz}\{(1-2\nu_I)^2Q^2 + 16(1-\nu_I)(1-2\nu_I)Q + 48(1-\nu_I)^2 \\
& - m_1[Q^2(1-2\nu_I)^2 + 2Q(1-2\nu_I)(2-3\nu_I) - 8(1-\nu_I^2)] \\
& + (1-2\nu_I)[-2m_1^2(1-\nu_I)(Q+2) - m_1^2 - m_1^3 - d_1^2(2Q\nu_I \\
& - 3 + 4\nu_I + m_1)]\} + \widetilde{B}^I_{zz}\{[-(1-2\nu_I)^2Q^2 - 6(1-2\nu_I)(1-\nu_I)Q \\
& - 8(1-\nu_I)(2-\nu_I)]d_1 - (1-2\nu_I)[2d_1m_1(Q - 2Q\nu_I + 4 - 4\nu_I) \\
& + d_1m_1^2 + d_1^3]\}, \\
X = {} & d_1^2 + [m_1 + (Q + 4 - 2Q\nu_I - 4\nu_I)]^2.
\end{aligned} \tag{18}
$$

B^I_{zz} is obtained by replacing $\widetilde{A}^I_{zz}$, $\widetilde{B}^I_{zz}$ and d_1 in H_A with $\widetilde{B}^I_{zz}$, $\widetilde{A}^I_{zz}$ and $-d_1$, respectively. C^I_{zz} is obtained by replacing $\widetilde{A}^I_{zz}$, $\widetilde{B}^I_{zz}$, m_1 and d_1 in H_A and X with $\widetilde{C}^I_{zz}$, $\widetilde{D}^I_{zz}$, m_2 and d_2, respectively, and D^I_{zz} is obtained by replacing $\widetilde{A}^I_{zz}$, $\widetilde{B}^I_{zz}$, m_1 and d_1 with $\widetilde{D}^I_{zz}$, $\widetilde{C}^I_{zz}$, m_2 and $-d_2$, respectively.

In the inhomogeneity and matrix, the elastic solutions are also given by Eqs. (5), (6) and (12) but with $Q = 0$, since their elastic moduli are constant. This means that $h_1 = 3, h_2 = 1$, $h_3 = -2, h_4 = -4, h_5 = 1, h_6 = -2$. The solutions in Eqs. (5), (6) and (12) as applied to the inhomogeneity and matrix are identified with the superscripts 1 and 2, respectively.

In the Cartesian coordinate system, the deviatoric solution in Eq. (6) under ε^*_{zz} has the following form:

$$
\begin{aligned}
u^I_x &= \frac{1}{2}U^I_r\left(3\frac{z^2}{r^2} - 1\right)\frac{x}{r} - 3U^I_\theta\frac{xz^2}{r^3}, \\
u^I_y &= \frac{1}{2}U^I_r\left(3\frac{z^2}{r^2} - 1\right)\frac{y}{r} - 3U^I_\theta\frac{yz^2}{r^3}, \\
u^I_z &= \frac{1}{2}U^I_r\left(3\frac{z^2}{r^2} - 1\right)\frac{z}{r} + 3U^I_\theta\left(1 - \frac{z^2}{r^2}\right)\frac{z}{r},
\end{aligned} \tag{19}
$$

where U^I_r and U^I_θ are given in Eq. (12) for the case of real roots of Eq. (9), or Eq. (16) for the case of complex roots. Thanks to the spherical symmetry of the inhomogeneity problem under consideration, the deviatoric solutions under ε^*_{xx} and ε^*_{yy} can be obtained by the simultaneous permutation of the subscripts and the coordinates x, y and z from the displacements in Eq. (19). This procedure can also be found in the paper of Duan et al. (2005). Thus, it will not be reproduced here. However, as can be seen from Eq. (19), the displacements under ε^*_{xx} and ε^*_{yy} will also contain the functions U^I_r and U^I_θ given in Eq. (12), but the subscript zz should be replaced by xx and yy, respectively.

Now the solutions under shear eigenstrains ε^*_{xy}, ε^*_{xz} and ε^*_{yz} will be sought. We consider first the solution under shear eigenstrain ε^*_{xy}. Following a procedure similar to those in the works of Christensen and Lo (1979), and Duan et al. (2005), namely, by assuming that the displacements contain some unknown functions of r and substituting them into the equilibrium equations to solve the unknown functions, the displacements for the graded

interphase in the spherical coordinate system can be obtained

$$u_r^I = \frac{3}{2} U_r^I(r) \sin^2\theta \sin 2\varphi,$$
$$u_\theta^I = \frac{3}{2} U_\theta^I(r) \sin 2\theta \sin 2\varphi,$$
$$u_\varphi^I = 3 U_\theta^I(r) \sin\theta \cos 2\varphi, \tag{20}$$

where $U_r^I(r)$ and $U_\theta^I(r)$ are obtained from Eq. (12) or (16) by replacing the subscript zz with xy. Wang and Jasiuk (1998) gave the elastic solution of a spherical inhomogeneity with an inhomogeneous interphase (with the power-law variation in elastic moduli) in an infinite matrix under non-vanishing remote shear stress σ_{xy}^0. Their solution is similar to those in Eq. (20). Luo and Weng (1987) gave the elastic solution of a spherical inhomogeneity with a homogeneous interphase in an infinite matrix under non-vanishing eigenstrains $\varepsilon_{xx}^* = -\varepsilon_{yy}^*$. Their solution can be obtained directly from Eqs. (20) after a $\pi/4$ coordinate transformation and setting $Q = 0$. Using the same procedure as above, we get the displacements under shear eigenstrain ε_{xz}^*

$$u_r^I = \frac{3}{2} U_r^I \sin 2\theta \cos\varphi, \quad u_\theta^I = 3 U_\theta^I \cos 2\theta \cos\varphi, \quad u_\varphi^I = -3 U_\theta^I \cos\theta \sin\varphi \tag{21}$$

and those under shear eigenstrain ε_{yz}^*

$$u_r^I = \frac{3}{2} U_r^I \sin 2\theta \sin\varphi, \quad u_\theta^I = 3 U_\theta^I \cos 2\theta \sin\varphi, \quad u_\varphi^I = 3 U_\theta^I \cos\theta \cos\varphi, \tag{22}$$

where $U_r^I(r)$ and $U_\theta^I(r)$ in Eqs. (21) and (22) are obtained from Eq. (12) or (16) by replacing the subscript zz with xz and yz, respectively.

We have obtained above the basic solutions under six different eigenstrains. Using the relations between the displacements and strains, and the Hooke's law, the stress fields can be obtained. The constants $A_{pq}^k, B_{pq}^k, C_{pq}^k, D_{pq}^k, F_{pp}^k$ and G_{pp}^k $(p, q = x, y, z)$ under six different eigenstrains are determined from the continuity and boundary conditions

$$\mathbf{u}^1 + \boldsymbol{\varepsilon}^* \cdot \mathbf{x} = \mathbf{u}^I, \quad \boldsymbol{\sigma}^1 \cdot \mathbf{N}_1 = \boldsymbol{\sigma}^I \cdot \mathbf{N}_1 \quad \text{at } \Gamma_{1I},$$
$$\mathbf{u}^I = \mathbf{u}^2, \quad \boldsymbol{\sigma}^I \cdot \mathbf{N}_2 = \boldsymbol{\sigma}^2 \cdot \mathbf{N}_2 \quad \text{at } \Gamma_{I2},$$
$$\mathbf{u}^2 = \mathbf{0}, \quad \boldsymbol{\sigma}^2 = \mathbf{0} \quad \text{at } r \to \infty, \tag{23}$$

where $\mathbf{N}_1$ and $\mathbf{N}_2$ are the unit normal vectors to Γ_{1I} and Γ_{I2}, respectively. It is found that under $\varepsilon_{xx}^* = 1, \varepsilon_{yy}^* = 1, \varepsilon_{zz}^* = 1, \varepsilon_{xy}^* = 1, \varepsilon_{xz}^* = 1$ and $\varepsilon_{yz}^* = 1$, respectively, the constants A_{pq}^k $(p, q = x, y, z)$ are equal for each of $k = 1, I, 2$, e.g., $A_{xx}^k = A_{yy}^k = A_{zz}^k = A_{xy}^k = A_{xz}^k = A_{yz}^k$. The constants B_{pq}^k, C_{pq}^k, D_{pq}^k, F_{pq}^k and G_{pq}^k also obey their own respective identities. Therefore, for brevity, we introduce constants A_k, B_k, C_k, D_k, F_k and G_k for the inhomogeneity and matrix (i.e. $k = 1, 2$) such that

$$A_k \equiv \frac{A_{pq}^k}{12\nu_k}, \quad B_k \equiv \frac{B_{pq}^k}{2}, \quad C_k \equiv \frac{C_{pq}^k}{2(5-4\nu_k)}, \quad D_k \equiv -\frac{D_{pq}^k}{3},$$
$$F_k \equiv F_{pp}^k, \; G_k \equiv G_{pp}^k, \tag{24}$$

where $pp = xx, yy, zz$ and $pq = xx, yy, zz, xy, xz, yz$ denote the loading cases $\varepsilon_{xx}^* \neq 0, \varepsilon_{yy}^* \neq 0$, $\varepsilon_{zz}^* \neq 0, \varepsilon_{xy}^* \neq 0, \varepsilon_{xz}^* \neq 0$ and $\varepsilon_{yz}^* \neq 0$, respectively. In the inhomogeneity $(k = 1)$, C_1, D_1 and G_1

vanish; in the matrix ($k=2$), A_2, B_2 and F_2 vanish. For the graded interphase we introduce constants M_i ($i=1,2,\ldots,6$) and N_j ($j=1,2,3,4$) such that

$$M_1 \equiv A^I_{pq}, \quad M_2 \equiv B^I_{pq}, \quad M_3 \equiv C^I_{pq}, \quad M_4 \equiv D^I_{pq}, \quad M_5 \equiv F^I_{pp},$$
$$M_6 \equiv G^I_{pp}, \quad N_1 \equiv \widetilde{A}^I_{pq}, \quad N_2 \equiv \widetilde{B}^I_{pq}, \quad N_3 \equiv \widetilde{C}^I_{pq}, \quad N_4 \equiv \widetilde{D}^I_{pq}. \tag{25}$$

From Eq. (25), it follows that the relations between M_i and N_i ($i=1,2,3,4$) obey Eq. (13) when the roots are real (e.g. homogeneous interphase), and Eqs. (17) and (18) when they are complex.

Therefore, the final elastic fields in the inhomogeneity and matrix contain the constants A_k, B_k, C_k, D_k, F_k and G_k ($k=1,2$), and those in the interphase the constants M_i ($i=1,2,\ldots,6$) and N_j ($j=1,2,3,4$). These constants are easily obtained from the corresponding continuity conditions and remote boundary conditions in Eq. (23), but the expressions are generally lengthy for the three-phase configuration of Fig. 1. Therefore, they are not reproduced here. Knowing these constants, the Eshelby tensors for the three phases can be calculated from the formulas given in the next section, where we shall also discuss their general properties. Detailed expressions for the constants for spherical *inhomogeneous inclusions* in finite domains will however be given in Section 4.

3. Eshelby tensors in three phases

The Eshelby tensors relate the total strains $\boldsymbol{\varepsilon}^k$ in the three phases to the prescribed uniform eigenstrain in the inhomogeneity, i.e.

$$\boldsymbol{\varepsilon}^k(\mathbf{r}) = \mathbf{S}^k(\mathbf{r}) : \boldsymbol{\varepsilon}^*, \quad (k=1,I,2). \tag{26}$$

Because of the geometrical and physical symmetry of the problem under consideration, the Eshelby tensors in the three phases are all transversely isotropic tensors with any of the radii being an axis of symmetry. Moreover, these Eshelby tensors here are generally position-dependent. Using the Walpole notation (Walpole, 1981) for transversely isotropic tensors, a fourth-order tensor $\mathbf{S}^k(\mathbf{r})$ with the above-mentioned radial symmetry can be expressed in a concise matrix form

$$\mathbf{S}^k(\mathbf{r}) = \widetilde{\mathbf{S}}^k(r) \cdot \widetilde{\mathbf{E}}^{\mathrm{T}}, \tag{27}$$

in which

$$\widetilde{\mathbf{S}}^k(r) = [\, S^k_1(r) \quad S^k_2(r) \quad S^k_3(r) \quad S^k_4(r) \quad S^k_5(r) \quad S^k_6(r) \,], \tag{28}$$

$$\widetilde{\mathbf{E}} = [\, \mathbf{E}^1 \quad \mathbf{E}^2 \quad \mathbf{E}^3 \quad \mathbf{E}^4 \quad \mathbf{E}^5 \quad \mathbf{E}^6 \,], \tag{29}$$

where $\mathbf{r}$ ($\mathbf{r}=r\mathbf{n}$) is the position vector. $\mathbf{n}=n_i\mathbf{e}_i$ is the unit vector along the radius passing the material point at which the Eshelby tensor is calculated. n_i is the direction cosine of $\mathbf{r}$ and $i=1,2,3$ denote x-, y- and z-directions, respectively. $S^k_p(r)$ ($p=1,2,\ldots,6$) are functions of r, and $\mathbf{E}^p$ ($p=1,2,\ldots,6$) are the six elementary tensors introduced by Walpole (1981).

From the elastic solutions in Section 2, the Eshelby tensors in the inhomogeneity and the matrix are given by Eq. (27) with $\widetilde{\mathbf{S}}^1(r)$ and $\widetilde{\mathbf{S}}^2(r)$ being

$$\widetilde{\mathbf{S}}^1(r) = \begin{bmatrix} 1+B_1+2F_1+3(7-8\nu_1)A_1r^2 \\ 1+2B_1+F_1+36\nu_1A_1r^2 \\ 1+3B_1+3(7-4\nu_1)A_1r^2 \\ 1+3B_1+3(7+2\nu_1)A_1r^2 \\ -B_1+F_1-18\nu_1A_1r^2 \\ -B_1+F_1-3(7-8\nu_1)A_1r^2 \end{bmatrix}^{\mathrm{T}}, \tag{30}$$

$$\widetilde{\mathbf{S}}^2(r) = \begin{bmatrix} 6D_2/r^5+2[G_2-2(1+\nu_2)C_2]/r^3 \\ 12D_2/r^5-2[G_2+2(5-4\nu_2)C_2]/r^3 \\ 3D_2/r^5+6C_2(1-2\nu_2)/r^3 \\ -12D_2/r^5+6C_2(1+\nu_2)/r^3 \\ -6D_2/r^5-2[G_2-(5-4\nu_2)C_2]/r^3 \\ -6D_2/r^5+[G_2+4(1+\nu_2)C_2]/r^3 \end{bmatrix}^{\mathrm{T}}, \tag{31}$$

where A_1, B_1, F_1, C_2, D_2 and G_2 are given in Eq. (24). The Eshelby tensor in the graded interphase has a more complicated form with $\widetilde{\mathbf{S}}^I(r)$ being

$$\widetilde{\mathbf{S}}^I(r) = -\frac{1}{2}\begin{bmatrix} \sum_{i=1}^{4} 2\lambda_i(c_i+e_i) - \sum_{i=5}^{6} 4\lambda_i M_i \\ \sum_{i=1}^{4} \lambda_i(c_i+2e_i+f_i+g_i+4k_i+l_i) - \sum_{i=5}^{6} 2\lambda_i h_i M_i \\ \sum_{i=1}^{4} 2\lambda_i e_i \\ \sum_{i=1}^{4} 2\lambda_i(e_i+k_i) \\ \sum_{i=1}^{4} \lambda_i\left(c_i+g_i\right) - \sum_{i=5}^{6} 2\lambda_i h_i M_i \\ \sum_{i=1}^{4} \lambda_i(c_i+f_i) - \sum_{i=5}^{6} 2\lambda_i M_i \end{bmatrix}^{\mathrm{T}}. \tag{32}$$

When the roots of Eq. (9) are real, λ_i, c_i, e_i, f_i, g_i, k_i and l_i $(i=1,2,3,4)$ in Eq. (32) are

$$\begin{aligned} &\lambda_i = r^{h_i-1} \quad (i=1,2,\ldots,6), \\ &c_i = M_i, \quad e_i = -3N_i, \quad f_i = -3M_i+6N_i, \quad g_i = M_i(h_i-1), \\ &k_i = -\tfrac{3}{2}[M_i+N_i(h_i-3)], \quad l_i = -3M_i(h_i-3)+6N_i(h_i-3). \end{aligned} \tag{33}$$

The constants M_i $(i=1,2,\ldots,6)$ and N_j $(j=1,2,3,4)$ are given in Eq. (25). When the roots are complex, λ_i in Eq. (32) are

$$\lambda_1 = r^{m_1-1}\cos(d_1\ln r),\quad \lambda_2 = r^{m_1-1}\sin(d_1\ln r),\quad \lambda_3 = r^{m_2-1}\cos(d_2\ln r),$$
$$\lambda_4 = r^{m_2-1}\sin(d_2\ln r),\quad \lambda_5 = r^{h_5-1},\quad \lambda_6 = r^{h_6-1}. \tag{34}$$

Then c_i, e_i, f_i, g_i, k_i and l_i $(i=1,2,3,4)$ are given below. For $i=1$

$$c_1 = M_1,\quad e_1 = -3N_1,\quad f_1 = -3M_1 + 6N_1,$$
$$g_1 = M_1(m_1-1) + M_2 d_1,\quad k_1 = -\tfrac{3}{2}[M_1 + N_1(m_1-3) + N_2 d_1],$$
$$l_1 = -3M_1(m_1-3) + 6N_1(m_1-3) - 3M_2 d_1 + 6N_2 d_1. \tag{35}$$

For $i=2$ the constants can be obtained by replacing M_1, N_1, M_2, N_2, m_1 and d_1 in Eq. (35) with M_2, N_2, M_1, N_1, m_1 and $-d_1$, respectively, for $i=3$ by replacing them with M_3, N_3, M_4, N_4, m_2 and d_2, respectively, and for $i=4$ with M_4, N_4, M_3, N_3, m_2 and $-d_2$, respectively.

When the interphase is homogeneous (non-graded, $Q=0$), $h_1=3, h_2=1, h_3=-2$, $h_4=-4, h_5=1, h_6=-2$. M_i and N_i $(i=1,2,3,4)$ are related to each other through

$$M_i = N_i\frac{[12-12\nu_I-(1-2\nu_I)(h_i+h_i^2)]}{(h_i+4-4\nu_I)},\quad (i=1,2,3,4). \tag{36}$$

For consistency with the expressions in Eqs. (30) and (31), for the homogeneous interphase, we introduce constants A_I, B_I, C_I, D_I, F_I and G_I. The relations between them and M_1, M_2, M_3, M_4, M_5 and M_6 in Eq. (25) are

$$A_I \equiv \frac{M_1}{12\nu_I},\quad B_I \equiv \frac{M_2}{2},\quad C_I \equiv \frac{M_3}{2(5-4\nu_I)},\quad D_I \equiv -\frac{M_4}{3},\quad F_I \equiv M_5,\quad G_I \equiv M_6. \tag{37}$$

Therefore, for the homogeneous interphase ($Q=0$), $\widetilde{\mathbf{S}}^I(r)$ is given by

$$\widetilde{\mathbf{S}}^I(r) = \begin{bmatrix} B_I + 2F_I + 3(7-8\nu_I)A_I r^2 + 2[G_I - 2(1+\nu_I)C_I]\frac{1}{r^3} + 6D_I\frac{1}{r^5} \\ 2B_I + F_I + 36\nu_I A_I r^2 - 2[G_I + 2(5-4\nu_I)C_I]\frac{1}{r^3} + 12D_I\frac{1}{r^5} \\ 3B_I + 3(7-4\nu_I)A_I r^2 + 6(1-2\nu_I)C_I\frac{1}{r^3} + 3D_I\frac{1}{r^5} \\ 3B_I + 3(7+2\nu_I)A_I r^2 + 6(1+\nu_I)C_I\frac{1}{r^3} - 12D_I\frac{1}{r^5} \\ -B_I + F_I - 18\nu_I A_I r^2 - 2[G_I - (5-4\nu_I)C_I]\frac{1}{r^3} - 6D_I\frac{1}{r^5} \\ -B_I + F_I - 3(7-8\nu_I)A_I r^2 + [G_I + 4(1+\nu_I)C_I]\frac{1}{r^3} - 6D_I\frac{1}{r^5} \end{bmatrix}^{\mathrm{T}}. \tag{38}$$

Under dilatational eigenstrain $\boldsymbol{\varepsilon}^* = \varepsilon_m^*\mathbf{I}^{(2)}$, the total strain in the inhomogeneity is given by $\boldsymbol{\varepsilon}^1 = \varepsilon_m^*\mathbf{S}^1 : \mathbf{I}^{(2)}$. It can be verified that $\mathbf{S}^1 : \mathbf{I}^{(2)}$ is a constant tensor and thus the stress field in the inhomogeneity is uniform even in the three-phase configuration with a graded interphase. If the inhomogeneity, the interphase and the matrix have the same elastic moduli, then the Eshelby tensors given in Eqs. (30) and (31) reduce to the classical interior and exterior Eshelby tensors for a spherical *inclusion*.

As we shall demonstrate in Section 7, the volume average Eshelby tensors can be used to predict the effective moduli of composites. Here, we give the volume average of the

Eshelby tensor for the spherical *inhomogeneous inclusion* in the studied three-phase model when the interphase is a (non-graded) homogeneous material. The average tensor is defined as

$$\bar{\mathbf{S}}^1 = \frac{1}{V_1}\int_{V_1} \widetilde{\mathbf{S}}^1(r)\cdot\widetilde{\mathbf{E}}^{\mathrm{T}}\,\mathrm{d}V, \tag{39}$$

where V_1 is the volume of the inhomogeneity. Performing the volume integration, it is found that $\bar{\mathbf{S}}^1$ is an isotropic tensor

$$\bar{\mathbf{S}}^1 = (1+3F_1)\mathbf{J} + \left(1+\frac{63A_1}{5}+3B_1\right)\mathbf{K}, \tag{40}$$

where

$$\mathbf{J} = \tfrac{1}{3}\mathbf{I}^{(2)}\otimes\mathbf{I}^{(2)}, \quad \mathbf{K} = -\tfrac{1}{3}\mathbf{I}^{(2)}\otimes\mathbf{I}^{(2)} + \mathbf{I}^{(4s)}, \tag{41}$$

with $\mathbf{I}^{(2)}$ and $\mathbf{I}^{(4s)}$ being the second- and fourth-order symmetric identity tensors, respectively. For an *inhomogeneous inclusion* with a non-graded interphase, the procedure for the solutions of the constants F_1, A_1 and B_1 has been depicted above. Their expressions will not be given here for they are lengthy. Instead, we give the detailed expressions for these constants when the spherical inhomogeneity has the same elastic constants as the interphase, namely, when the *inhomogeneous inclusion* degenerates into an *inclusion* in a spherical region which, in turn, is embedded in an alien infinite matrix. In this case, $g_{1I} = \mu_1/\mu_I = 1$, $g_{2I} = \mu_2/\mu_I = g_{21} = \mu_2/\mu_1$ and $v_1 = v_I$, and the infinite matrix material has different elastic moduli. Then the constants F_1, A_1 and B_1 are

$$\begin{aligned}
F_1 &= -\frac{2(1-2v_1)}{3H_1}\{[1-\rho^3(1-g_{21})](1+v_1) - 4g_{21}v_1 + 2g_{21}\},\\
A_1 &= \frac{2(1-\rho^2)\rho^5(1-g_{21})}{H_2},\\
B_1 &= \frac{2\rho^3 H_{12}}{15H_2[-8-7g_{21}+5(2+g_{21})v_2]} - \frac{7-5v_1}{45-45v_1},
\end{aligned} \tag{42}$$

with $\rho = a/b$ and

$$\begin{aligned}
H_1 &= 3(1-v_1)[1+2g_{21}+(1-4g_{21})v_1],\\
H_2 &= 3(1-v_1)[7(1+4g_{21})+5(1-8g_{21})v_1],\\
H_{12} &= (200v_1^2 - 300v_1 - 63\rho^2 + 175)(7-5v_2)g_{21}^2 + 3g_{21}\{75v_1(7-9v_2)\\
&\quad - 25v_1^2(13-15v_2) - 7[25+3\rho^2-5(5+3\rho^2)v_2]\}\\
&\quad + (4-5v_2)(25v_1^2 + 126\rho^2 - 175).
\end{aligned} \tag{43}$$

When $g_{21} = 1$, $v_1 = v_2$ and $\rho = 1$, $\mathbf{S}^1$ in Eq. (27) and $\bar{\mathbf{S}}^1$ in Eq. (40) degenerate into the classical Eshelby tensor, denoted by $\mathbf{S}^0$, for a spherical *inclusion* in an infinite homogeneous medium.

4. Eshelby tensors in finite domains

4.1. Fixed displacement boundary condition

Letting the moduli of the infinite matrix in the three-phase problem in Section 3 tend to infinity, we obtain the solution for a spherical *inhomogeneous inclusion* in a finite domain whose outer boundary is fixed. In this case, when the shell is homogeneous ($Q=0$), the Eshelby tensors in the finite domain are given through Eqs. (27), (30) and (38), and the constants $A_1, B_1, F_1, A_I, B_I, C_I, D_I, F_I$ and G_I are

$$
\begin{aligned}
&F_1 = -\frac{(1-2\nu_1)[2+\rho^3-(4-\rho^3)\nu_I]}{W_1}, \quad A_1 = \frac{175 g_{1I}\rho^5(1-\rho^2)(1-\nu_I)}{W_2},\\
&B_1 = \frac{W_3}{3W_2}, \quad F_I = -\frac{\rho^3 g_{1I}(1+\nu_1)(1-2\nu_I)}{W_1}, \quad G_I = -\frac{F_I}{\rho^3},\\
&A_I = \frac{5g_{1I}\rho^5(1-\rho^2)}{W_2}[28-40\nu_1+g_{1I}(7+5\nu_1)], \quad B_I = \frac{\rho^3 g_{1I} W_4}{3W_2},\\
&C_I = \frac{5g_{1I}}{3W_2}[W_5\rho^7 - W_6(7-10\nu_I)], \quad D_I = \frac{2g_{1I}}{W_2}[W_5\rho^5 - W_6(7-10\nu_I)],
\end{aligned}
\tag{44}
$$

where $g_{1I}=\mu_1/\mu_I$ and W_i $(i=1,2,\ldots,6)$ are

$$
\begin{aligned}
W_1 &= 3g_{1I}(1-\rho^3)(1+\nu_1)(1-2\nu_I) + 3(1-2\nu_1)[2+\rho^3-(4-\rho^3)\nu_I],\\
W_2 &= 4(1-g_{1I})(4-5\nu_I)W_5\rho^{10} + 25W_7\rho^7 + (1-g_{1I})W_6[126\rho^5\\
&\quad - 25(7-12\nu_I+8\nu_I^2)\rho^3] + 2W_6(7-10\nu_I)[-7+5\nu_I-2g_{1I}(4-5\nu_I)],\\
W_3 &= -4(4-5\nu_I)W_5\rho^{10} + 25W_8\rho^7 + 63W_9\rho^5 + 25W_6(7-12\nu_I+8\nu_I^2)\rho^3\\
&\quad + 2W_6(49-105\nu_I+50\nu_I^2),\\
W_4 &= -4(4-5\nu_I)W_5\rho^7 - W_6(-175+63\rho^2+300\nu_I-200\nu_I^2),\\
W_5 &= (7-10\nu_1)(7+5\nu_I) - g_{1I}(7+5\nu_1)(7-10\nu_I),\\
W_6 &= -28+40\nu_1 - g_{1I}(7+5\nu_1),
\end{aligned}
\tag{45}
$$

with

$$
\begin{aligned}
W_7 &= 2(7-10\nu_1)(7-\nu_I^2) - g_{1I}^2(7+5\nu_1)(7-12\nu_I+8\nu_I^2)\\
&\quad + g_{1I}[-7(7-6\nu_I+8\nu_I^2) + \nu_1(49+66\nu_I+20\nu_I^2)],\\
W_8 &= -2(7-10\nu_1)(7-\nu_I^2) + g_{1I}[7(14-21\nu_I+4\nu_I^2) + \nu_1(7-42\nu_I+20\nu_I^2)],\\
W_9 &= -2W_6 - 35g_{1I}(1-\nu_I).
\end{aligned}
\tag{46}
$$

When the inhomogeneity and the homogeneous shell have the same elastic moduli ($g_{1I}=1, \nu_1=\nu_I$), the solution reduces to that of a spherical *inclusion* in a finite domain.

4.2. Traction-free boundary condition

Letting the moduli of the infinite matrix in the three-phase configuration in Fig. 1 vanish, we obtain the solution for a spherical inhomogeneity in a finite domain with a traction-free boundary condition. In this case, when the shell is homogeneous ($Q=0$), the Eshelby tensors in the finite domain are given through Eqs. (27), (30) and (38), and the

constants $A_1, B_1, F_1, A_I, B_I, C_I, D_I, F_I$ and G_I are

$$
\begin{aligned}
&F_1 = \frac{2(1-\rho^3)(1-2\nu_1)(1+\nu_I)}{W_{10}}, \quad A_1 = -\frac{350\rho^5 g_{1I}(1-\rho^2)(1-\nu_I)}{W_{11}},\\
&B_1 = \frac{W_{12}}{3W_{11}}, \quad F_I = -\frac{2\rho^3 g_{1I}(1-2\nu_I)(1+\nu_1)}{W_{10}}, \quad G_I = \frac{F_I(1+\nu_I)}{2\rho^3(1-2\nu_I)},\\
&A_I = -\frac{10\rho^5 g_{1I}(1-\rho^2)[7(4+g_{1I})-5(8-g_{1I})\nu_1]}{W_{11}}, \quad B_I = \frac{\rho^3 g_{1I} W_{13}}{3W_{11}},\\
&C_I = -\frac{5g_{1I}}{6W_{11}}[4W_5\rho^7 + W_6(7+5\nu_I)], \quad D_I = -\frac{g_{1I}}{W_{11}}[4W_5\rho^5 + W_6(7+5\nu_I)],
\end{aligned} \tag{47}
$$

where W_5 and W_6 are given in Eq. (45), and W_n ($n = 10, 11, 12, 13$) are

$$
\begin{aligned}
W_{10} =& -6(1-\rho^3)(1-2\nu_1)(1+\nu_I) - 3g_{1I}(1+\nu_1)[1+2\rho^3+(1-4\rho^3)\nu_I],\\
W_{11} =& 4(1-g_{1I})(7-5\nu_I)W_5\rho^{10} + 50W_{15}\rho^7 - 252(1-g_{1I})W_6\rho^5\\
&+ 25(1-g_{1I})(7-\nu_I^2)W_6\rho^3 + W_6(7+5\nu_I)[-7-8g_{1I}+5(1+2g_{1I})\nu_I],\\
W_{12} =& -4(7-5\nu_I)W_5\rho^{10} - 50W_{14}\rho^7 - 25(7-\nu_I^2)W_6\rho^3\\
&+ (49-25\nu_I^2)W_6 - 126[-10(8-g_{1I})\nu_1 + 7(8-3g_{1I}+5g_{1I}\nu_I)]\rho^5,\\
W_{13} =& -4(7-5\nu_I)W_5\rho^7 + 126W_6\rho^2 - 25W_6(7-\nu_I^2),
\end{aligned} \tag{48}
$$

with

$$
\begin{aligned}
W_{14} =& \nu_1[7(20+g_{1I}) - 42g_{1I}\nu_I - 20(1-g_{1I})\nu_I^2]\\
&- 7[14(1-g_{1I}) + 21g_{1I}\nu_I - 2(1+2g_{1I})\nu_I^2],\\
W_{15} =& 7[7(-2+g_{1I}+g_{1I}^2) - 6g_{1I}(1+2g_{1I})\nu_I + 2(1+2g_{1I})^2\nu_I^2]\\
&+ \nu_1[7(20-7g_{1I}+5g_{1I}^2) - 6g_{1I}(11+10g_{1I})\nu_I - 20(1+g_{1I}-2g_{1I}^2)\nu_I^2].
\end{aligned} \tag{49}
$$

When the inhomogeneity and the homogeneous shell have the same elastic moduli, i.e. $g_{1I} = 1, \nu_1 = \nu_I$, the solution reduces to that of a spherical *inclusion* in a free finite domain.

It is noted that Li et al. (2005), and Wang et al. (2005) recently solved the circular and spherical *inclusion* problems in finite circular and spherical regions with fixed displacement or traction-free boundary conditions, and gave the corresponding Eshelby tensors. The present solutions are different from those of Li et al. (2005), and Wang et al. (2005) in that the former are for *inhomogeneous inclusions*.

5. Stress concentration tensors in three phases

In this section, we solve the elastic field in the three-phase region shown in Fig. 1 when a uniform stress field $\boldsymbol{\sigma}^0$ is prescribed at infinity. It is noted that previously, Herve and Zaoui (1993) have solved the elastic field in an infinite medium containing a spherical inhomogeneity with multiple homogeneous shells. Here, like the case for a general

eigenstrain, the solution for a general remote stress $\boldsymbol{\sigma}^0$ is also obtained by superposition. Under the respective remote loadings $\sigma^0_{xx}\neq 0, \sigma^0_{yy}\neq 0, \sigma^0_{zz}\neq 0, \sigma^0_{xy}\neq 0, \sigma^0_{xz}\neq 0$ and $\sigma^0_{yz}\neq 0$, the elastic solutions have the same forms as those under the corresponding eigenstrains. However, the usual stress and displacement continuity conditions at Γ_{1I} and Γ_{I2} and the remote boundary conditions should be satisfied. It is found that under $\sigma^0_{xx}=1, \sigma^0_{yy}=1$, $\sigma^0_{zz}=1, \sigma^0_{xy}=1, \sigma^0_{xz}=1$ and $\sigma^0_{yz}=1$, respectively, the constants $A^k_{pq}, B^k_{pq}, C^k_{pq}, D^k_{pq}, F^k_{pp}$ and G^k_{pp} $(p,q=x,y,z)$ in Eqs. (5), (6), (12) and (16) for the inhomogeneity (superscript 1), the graded interphase (superscript I) and the matrix (superscript 2) still obey the identities like $A^k_{xx}=A^k_{yy}=A^k_{zz}=A^k_{xy}=A^k_{xz}=A^k_{yz}$. Thus, we introduce constants A_k, B_k, C_k, D_k, F_k and G_k $(k=1,2)$ for the inhomogeneity and matrix such that

$$\begin{aligned}
&12\nu_k A_k\sigma^0_{pq}\equiv\mu_k A^k_{pq},\quad 2B_k\sigma^0_{pq}\equiv\mu_k B^k_{pq},\quad 2(5-4\nu_k)C_k\sigma^0_{pq}\equiv\mu_k C^k_{pq},\\
&-3D_k\sigma^0_{pq}\equiv\mu_k D^k_{pq},\quad F_k\sigma^0_{pp}\equiv\frac{2(1+\nu_k)}{1-2\nu_k}\mu_k F^k_{pp},\quad G_k\sigma^0_{pp}\equiv\mu_k G^k_{pp},
\end{aligned}\tag{50}$$

where $p,q=x,y,z$ denote different loading cases. In the inhomogeneity $(k=1)$, C_1, D_1 and G_1 vanish; in the matrix $(k=2)$, A_2 and F_2 vanish. For the graded interphase we introduce constants M_i $(i=1,2,\ldots,6)$ and N_j $(j=1,2,3,4)$ such that

$$\begin{aligned}
&M_1\sigma^0_{pq}\equiv\mu_I A^I_{pq},\quad M_2\sigma^0_{pq}\equiv\mu_I B^I_{pq},\quad M_3\sigma^0_{pq}\equiv\mu_I C^I_{pq},\quad M_4\sigma^0_{pq}\equiv\mu_I D^I_{pq},\\
&N_1\sigma^0_{pq}\equiv\mu_I \widetilde{A}^I_{pq},\quad N_2\sigma^0_{pq}\equiv\mu_I \widetilde{B}^I_{pq},\quad N_3\sigma^0_{pq}\equiv\mu_I \widetilde{C}^I_{pq},\quad N_4\sigma^0_{pq}\equiv\mu_I \widetilde{D}^I_{pq},\\
&M_5\sigma^0_{pp}\equiv\mu_I F^I_{pp},\quad M_6\sigma^0_{pp}\equiv\mu_I G^I_{pp}.
\end{aligned}\tag{51}$$

From Eq. (51), it follows that the constants M_i and N_i $(i=1,2,3,4)$ obey Eq. (13) when the roots of Eq. (9) are real (e.g. homogeneous interphase), and Eqs. (17) and (18) when they are complex. Therefore, the final elastic fields in the inhomogeneity and matrix contain the constants A_k, B_k, C_k, D_k, F_k and G_k $(k=1,2)$, and those in the interphase the constants M_i $(i=1,2,\ldots,6)$ and N_j $(j=1,2,3,4)$. These constants are easily obtained from the corresponding continuity conditions and remote boundary conditions.

The stress concentration tensors $\mathbf{T}^k(\mathbf{x})$ $(k=1,I,2)$ relate the total stresses $\boldsymbol{\sigma}^k(\mathbf{x})$ in the three phases to the prescribed uniform remote stress $\boldsymbol{\sigma}^0$,

$$\boldsymbol{\sigma}^k=\mathbf{T}^k(\mathbf{r}):\boldsymbol{\sigma}^0,\quad (k=1,I,2).\tag{52}$$

The stress concentration tensors have the same properties as those of the Eshelby tensors; therefore, $\mathbf{T}^k(\mathbf{r})$ can be expressed as follows:

$$\mathbf{T}^k(\mathbf{r})=\widetilde{\mathbf{T}}^k(r)\cdot\widetilde{\mathbf{E}}^{\mathrm{T}},\tag{53}$$

where

$$\widetilde{\mathbf{T}}^k(r)=[\,T^k_1(r)\quad T^k_2(r)\quad T^k_3(r)\quad T^k_4(r)\quad T^k_5(r)\quad T^k_6(r)\,].\tag{54}$$

In the inhomogeneity, $\widetilde{\mathbf{T}}^1(r)$ is

$$\widetilde{\mathbf{T}}^1(r)=\begin{bmatrix} 2B_1+2F_1+6(7+6\nu_1)A_1r^2 \\ 4B_1+F_1-12\nu_1A_1r^2 \\ 6B_1+6(7-4\nu_1)A_1r^2 \\ 6B_1+6(7+2\nu_1)A_1r^2 \\ -2B_1+F_1+6\nu_1A_1r^2 \\ -2B_1+F_1-6(7+6\nu_1)A_1r^2 \end{bmatrix}^{\mathrm{T}}. \tag{55}$$

In the matrix, $\widetilde{\mathbf{T}}^2(r)$ is

$$\widetilde{\mathbf{T}}^2(r)=\begin{bmatrix} 1+12D_2/r^5+4[G_2-2(1-2\nu_2)C_2]/r^3 \\ 1+24D_2/r^5-4[G_2+2(5-\nu_2)C_2]/r^3 \\ 1+6D_2/r^5+12C_2(1-2\nu_2)/r^3 \\ 1-24D_2/r^5+12C_2(1+\nu_2)/r^3 \\ -12D_2/r^5-4[G_2-(5-\nu_2)C_2]/r^3 \\ -12D_2/r^5+2[G_2+4(1-2\nu_2)C_2]/r^3 \end{bmatrix}^{\mathrm{T}}. \tag{56}$$

In the inhomogeneous interphase, $\widetilde{\mathbf{T}}^I(r)$ is

$$\widetilde{\mathbf{T}}^I(r)=\begin{bmatrix} \sum_{i=1}^{4}2\lambda_i(c_i+e_i)+\sum_{i=5}^{6}4\lambda_i\frac{(1+h_i\nu_2)}{1-2\nu_2}M_i \\ \sum_{i=1}^{4}\lambda_i(c_i+2e_i+f_i+g_i+4k_i+l_i)+\sum_{i=5}^{6}2\lambda_i\frac{[h_i+(2-h_i)\nu_2]}{1-2\nu_2}M_i \\ \sum_{i=1}^{4}2\lambda_ie_i \\ \sum_{i=1}^{4}2\lambda_i(e_i+k_i) \\ \sum_{i=1}^{4}\lambda_i(c_i+g_i)+\sum_{i=5}^{6}2\lambda_i\frac{[h_i+(2-h_i)\nu_2]}{1-2\nu_2}M_i \\ \sum_{i=1}^{4}\lambda_i(c_i+f_i)+\sum_{i=5}^{6}2\lambda_i\frac{(1+h_i\nu_2)}{1-2\nu_2}M_i \end{bmatrix}^{\mathrm{T}}. \tag{57}$$

When the roots of Eq. (9) are real, λ_i is given by Eq. (33), and the other constants are

$$\begin{aligned} c_i&=\frac{1}{-1+2\nu_I}[(1+h_i\nu_I)M_i-6\nu_IN_i],\quad e_i=3N_i,\\ f_i&=\frac{1}{-1+2\nu_I}[-3(1+h_i\nu_I)M_i+6(1+\nu_I)N_i],\\ g_i&=-(h_i-1)M_i,\quad k_i=\tfrac{3}{2}[M_i+(h_i-3)N_i],\\ l_i&=-(9-3h_i)M_i-6(h_i-3)N_i. \end{aligned} \tag{58}$$

When the roots are complex (two pairs of complex conjugate roots), λ_i $(i=1,2,\ldots,6)$ are given by Eq. (34). For $i=1$,

$$
\begin{aligned}
&c_1=\frac{1}{-1+2\nu_I}[(1+m_1\nu_I)M_1-6\nu_I N_1+\nu_I M_2 d_1],\quad e_1=3N_1,\\
&f_1=\frac{1}{-1+2\nu_I}[-3(1+m_1\nu_I)M_1+6(1+\nu_I)N_1-3\nu_I M_2 d_1],\\
&g_1=-(m_1-1)M_1-M_2 d_1,\quad k_1=\tfrac{3}{2}[M_1+(m_1-3)N_1+N_2 d_1],\\
&l_1=-(9-3m_1)M_1-6(m_1-3)N_1+3M_2 d_1-6N_2 d_1.
\end{aligned}
\tag{59}
$$

For $i=2$, the constants can be obtained by replacing M_1, N_1, M_2, N_2, m_1 and d_1 in Eq. (59) with M_2, N_2, M_1, N_1, m_1 and $-d_1$, respectively, for $i=3$ by replacing them with M_3, N_3, M_4, N_4, m_2 and d_2, respectively, and for $i=4$ with M_4, N_4, M_3, N_3, m_2 and $-d_2$, respectively.

When the interphase is homogeneous ($Q=0$), $h_1=3, h_2=1, h_3=-2, h_4=-4, h_5=1$, $h_6=-2$. For consistency with the expressions in Eqs. (55) and (56), we introduce constants A_I, B_I, C_I, D_I, F_I and G_I such that

$$
\begin{aligned}
&12\nu_I A_I\equiv M_1,\quad 2B_I\equiv M_2,\quad 2(5-4\nu_k)C_I\equiv M_3,\\
&-3D_I\equiv M_4,\quad F_I\equiv\frac{2(1+\nu_I)}{1-2\nu_I}M_5,\quad G_I\equiv M_6.
\end{aligned}
\tag{60}
$$

Therefore, for the homogeneous interphase ($Q=0$), $\widetilde{\mathbf{T}}^I(r)$ is given by

$$
\widetilde{\mathbf{T}}^I(r)=\begin{bmatrix}
2B_I+2F_I+6(7+6\nu_I)A_I r^2+12D_I\frac{1}{r^5}+4[G_I-2(1-2\nu_I)C_I]\frac{1}{r^3}\\
4B_I+F_I-12\nu_I A_I r^2+24D_I\frac{1}{r^5}-4[G_I+2(5-\nu_I)C_I]\frac{1}{r^3}\\
6B_I+6(7-4\nu_I)A_I r^2+6D_I\frac{1}{r^5}+12(1-2\nu_I)C_I\frac{1}{r^3}\\
6B_I+6(7+2\nu_I)A_I r^2-24D_I\frac{1}{r^5}+12(1+\nu_I)C_I\frac{1}{r^3}\\
-2B_I+F_I+6\nu_I A_I r^2-12D_I\frac{1}{r^5}-4[G_I-(5-\nu_I)C_I]\frac{1}{r^3}\\
-2B_I+F_I-6(7+6\nu_I)A_I r^2-12D_I\frac{1}{r^5}+2[G_I+4(1-2\nu_I)C_I]\frac{1}{r^3}
\end{bmatrix}^{\mathrm{T}}.
\tag{61}
$$

The volume average of the stress concentration tensor $\bar{\mathbf{T}}^1$ for the inhomogeneity, which is useful in micromechanical approaches, is given by

$$
\bar{\mathbf{T}}^1=\frac{1}{V_1}\int_{V_1}\widetilde{\mathbf{T}}^1(r)\cdot\widetilde{\mathbf{E}}^{\mathrm{T}}\,\mathrm{d}V=3F_1\mathbf{J}+\frac{6}{5}(21A_1+5B_1)\mathbf{K}.
\tag{62}
$$

When $g_{1I}=1$ and $\nu_I=\nu_1$, $\mathbf{T}^1$ in Eq. (53) and $\bar{\mathbf{T}}^1$ in Eq. (62) degenerate into the classical stress concentration tensor $\mathbf{T}^0$ for a spherical inhomogeneity embedded in an alien infinite matrix.

6. Strain distributions in core–shell nanoparticles

A core–shell nanoparticle is usually composed of two different materials, e.g. CdSe coated CdS, ZnS coated CdSe, ZnSe coated CdSe, and CdS coated CdSe, etc. Many core–shell nanoparticles are nearly spherical and have a diameter of a few (3–5) (Danek et al., 1996; Peng et al., 1997; Dabbousi et al., 1997) to 11 nanometres (Kim et al., 2005). Because of the mismatch of the lattices of the materials, significant mismatch strains may

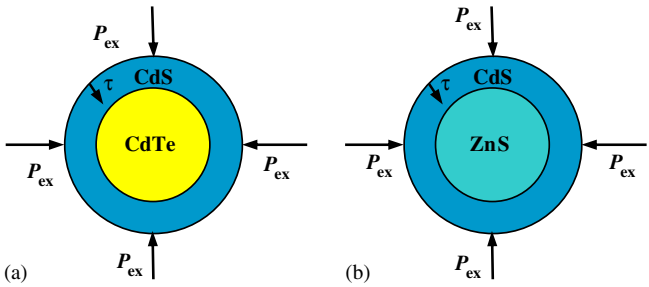

Fig. 2. (a) CdTe/CdS core–shell particle; (b) ZnS/CdS core–shell particle.

develop in core–shell nanoparticles (e.g. Rockenberger et al., 1998; Little et al., 2001). The lattice mismatch strain and the thermal strain can be treated as eigenstrains. In addition to the lattice mismatch, the large surface stress and applied external pressure can also produce a substantial lattice contraction (Little et al., 2001; Itskevich et al., 1998). In this section, we will use the Eshelby tensors in the finite domain with the traction-free boundary condition to analyze the elastic strain field in a core–shell particle under an eigenstrain $\boldsymbol{\varepsilon}^*$, a uniform and isotropic surface stress τ and external hydrostatic loading P_{ex}, as shown in Figs. 2(a) and (b). The strain field in the core and shell can be obtained by using the Eshelby tensors in Eqs. (27), (30) and (38) for an arbitrary uniform eigenstrain prescribed in the core, with the constants $A_1, B_1, F_1, A_I, B_I, C_I, D_I, F_I$ and G_I given in Eqs. (47) and (48). The elastic strain tensors $\boldsymbol{\varepsilon}^1_{\text{el}}$ and $\boldsymbol{\varepsilon}^I_{\text{el}}$ in the core and shell induced by $\boldsymbol{\varepsilon}^*$, τ and P_{ex} are

$$\boldsymbol{\varepsilon}^1_{\text{el}} = \mathbf{S}^1 : \boldsymbol{\varepsilon}^* - \boldsymbol{\varepsilon}^* + \boldsymbol{\varepsilon}^1(\tau, P_{\text{ex}}), \quad \boldsymbol{\varepsilon}^I_{\text{el}} = \mathbf{S}^I : \boldsymbol{\varepsilon}^* + \boldsymbol{\varepsilon}^I(\tau, P_{\text{ex}}), \tag{63}$$

where $\mathbf{S}^1$ and $\mathbf{S}^I$ are the Eshelby tensors in the core and shell, and they are given in Eqs. (27), (30) and (38). $\boldsymbol{\varepsilon}^1(\tau, P_{\text{ex}})$ and $\boldsymbol{\varepsilon}^I(\tau, P_{\text{ex}})$ in Eq. (63) are the elastic strain tensors in the core and shell due to τ and P_{ex}. The components of $\boldsymbol{\varepsilon}^1(\tau, P_{\text{ex}})$ and $\boldsymbol{\varepsilon}^I(\tau, P_{\text{ex}})$ in the spherical coordinate system are

$$\begin{aligned}
&\varepsilon^1_{rr}(\tau, P_{\text{ex}}) = \varepsilon^1_{\theta\theta}(\tau, P_{\text{ex}}) = \varepsilon^1_{\varphi\varphi}(\tau, P_{\text{ex}}) = -\frac{\mu_I(3\kappa_I + 4\mu_I)}{3\chi}\left(2\tau^* + \frac{P_{\text{ex}}}{\mu_I}\right),\\
&\varepsilon^I_{rr}(\tau, P_{\text{ex}}) = \Lambda_1 - \frac{2\Lambda_2}{r^3}, \quad \varepsilon^I_{\theta\theta}(\tau, P_{\text{ex}}) = \varepsilon^I_{\varphi\varphi}(\tau, P_{\text{ex}}) = \Lambda_1 + \frac{\Lambda_2}{r^3},
\end{aligned} \tag{64}$$

where $\tau^* = \tau/(b\mu_I)$, and

$$\begin{aligned}
&\chi = 4(1-\rho^3)\kappa_I\mu_I + \kappa_1(3\kappa_I + 4\rho^3\mu_I),\\
&\Lambda_1 = -\frac{\mu_I(3\kappa_1 + 4\mu_I)}{3\chi}\left(2\tau^* + \frac{P_{\text{ex}}}{\mu_I}\right), \quad \Lambda_2 = \frac{\mu_I(\kappa_1 - \kappa_I)}{\chi}\left(2\tau^* + \frac{P_{\text{ex}}}{\mu_I}\right).
\end{aligned} \tag{65}$$

Rockenberger et al. (1998) calculated the elastic strain distribution in the CdS coated CdTe core–shell system (CdTe/CdS, Fig. 2(a)) due to a dilatational eigenstrain $\boldsymbol{\varepsilon}^* = \varepsilon^*_m \mathbf{I}^{(2)}$ by assuming that the elastic constants of the CdTe core and CdS shell are the same within the framework of continuum mechanics. In order to compare our results with those of Rockenberger et al. (1998), we consider the strain field induced by a dilatational eigenstrain $\boldsymbol{\varepsilon}^* = \varepsilon^*_m \mathbf{I}^{(2)}$. For the core–shell structure, the misfit strain induced by the different lattice constants of the core and shell is $\varepsilon^*_m = (a_{\text{co}} - a_{\text{sh}})/a_{\text{sh}}$, where a_{co} and a_{sh} are

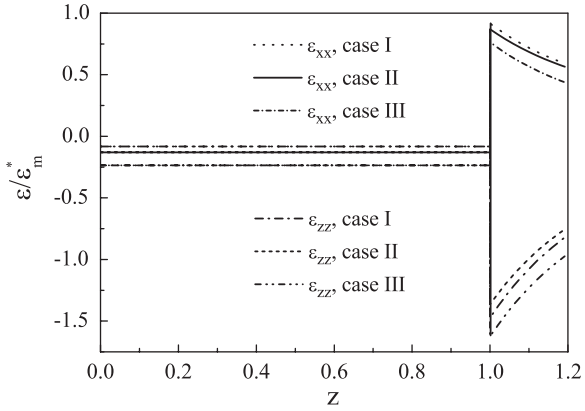

Fig. 3. Distributions of normalized elastic strains $\varepsilon_{zz}/\varepsilon_m^*$ and $\varepsilon_{xx}/\varepsilon_m^*$ in a CdTe/CdS core–shell nanoparticle subjected to ε_m^* and τ. It is noted that the core ($0 \leqslant z \leqslant 1.0$) is under hydrostatic compression. Thus, the curves of ε_{xx} and ε_{zz} merge into one in the core for each of the three cases.

the lattice constants of the core and shell, respectively. For example, the misfit strains are 11.6% for the CdTe/CdS core–shell structure and −7.0% for ZnS/CdS (Fig. 2(b)). Here, we give the numerical results for the CdTe/CdS nanoparticle for three cases: (I) The core and the shell have the same elastic constants with an eigenstrain $\varepsilon_m^* \mathbf{I}^{(2)}$ in the core; (II) The core and the shell have different elastic constants with an eigenstrain strain $\varepsilon_m^* \mathbf{I}^{(2)}$ in the core; (III) A surface stress τ on the outer surface of the particle is superimposed on the strain field of case (I). For the CdTe/CdS core–shell system, the outer radius r_{sh} of the nanoparticle is 0.9 nm with $\rho = 0.84$ (Rockenberger et al., 1998). The elastic strains ε_{xx} ($\varepsilon_{xx} = \varepsilon_{yy}$) and ε_{zz} along the z-axis (a radius) are plotted in Fig. 3. It is found that for this material combination the assumption that the core and the shell have the same elastic constants generates a relative difference $(\varepsilon(\mathrm{II}) - \varepsilon(\mathrm{I}))/\varepsilon(\mathrm{I}) = 56\%$ of the strain in the core, because the elastic constants of CdTe (bulk modulus 41.9 GPa, Poisson ratio 0.41) and CdS (bulk modulus 62.3 GPa, Poisson ratio 0.4) are different. Therefore, the difference in the elastic constants results in a significant difference in the strain field, which may have great effect on the physical properties. If we assume that there is a surface stress $\tau = 1\,\mathrm{N/m}$, then the effect of the surface stress on the magnitude of the strains is remarkable, and it may cause a substantial lattice contraction. The CdTe core is under hydrostatic compression, and the CdS shell is under biaxial tension in the tangential directions and compression in the radial direction.

7. Micromechanical scheme based on Eshelby and stress concentration tensors of three-phase configuration

Many micromechanical schemes have been developed to predict the effective elastic constants of linear composites (e.g. Aboudi, 1991; Bornert et al., 1996; Nemat-Nasser and Hori, 1999; Torquato, 2002; Milton, 2002). The framework for predicting the effective properties of nonlinear composites has also been well developed (Talbot and Willis, 1985; Pontecastaeda and Suquet, 1998; Willis, 2000). The work of Segurado and LLorca (2002) for linear composites containing non-overlapping identical spheres showed that for rigid spheres, Torquato's third-order approximation (TOA, Torquato, 1998) gives the effective

moduli closest to the numerical computation; for a glass-sphere/epoxy composite, the predictions of the generalized self-consistent method (GSCM, Christensen and Lo, 1979) and the TOA are practically identical, and they are very close to the numerical computation; and for spherical voids, the GSCM, the TOA and the numerical computation give practically identical results. In this case, the prediction of the Mori–Tanaka method (MTM, Mori and Tanaka, 1973; Benveniste, 1987) is also very close to the other two theoretical schemes and the numerical computation. However, it is noted that the MTM may severely underestimate the effective shear moduli of composites containing hard inhomogeneities, especially at large volume fractions, as is shown in the papers of Segurado and LLorca (2002), and Ma et al. (2004). It would therefore appear that from an overall point of view, the GSCM and the TOA tend to give the best results. It is noted that the three-phase model (GSCM) takes into account the matrix atmosphere, which is important in the prediction of the effective properties (Zheng and Du, 2001). Therefore, in this section, using the three-phase configuration in Fig. 1, we propose a micromechanical scheme to predict the effective moduli of composites containing spherical particles based upon the solutions of the inhomogeneity problems obtained in the previous sections.

We consider a two-phase composite composed of a continuous matrix and randomly distributed spherical particles. The effective stiffness tensor $\mathbf{C}^*$ and compliance tensor $\mathbf{D}^*$ of the composite can be calculated from the following expressions (Hill, 1963):

$$\mathbf{C}^* = \mathbf{C}_2 + f(\mathbf{C}_1 - \mathbf{C}_2) : \bar{\mathbf{E}}^1, \tag{66}$$

$$\mathbf{D}^* = \mathbf{D}_2 + f(\mathbf{D}_1 - \mathbf{D}_2) : \bar{\mathbf{T}}^1, \tag{67}$$

where $\mathbf{C}_1$ and $\mathbf{D}_1$ denote the stiffness and compliance tensors of the particles, respectively, and $\mathbf{C}_2$ and $\mathbf{D}_2$ those of the matrix. f is the volume fraction of the particles. $\bar{\mathbf{E}}^1$ in Eq. (66) is the strain concentration tensor in a particle, and $\bar{\mathbf{T}}^1$ in Eq. (67) is the stress concentration tensor. They are defined as

$$\bar{\boldsymbol{\varepsilon}}^1 = \bar{\mathbf{E}}^1 : \boldsymbol{\varepsilon}^0, \quad \bar{\boldsymbol{\sigma}}^1 = \bar{\mathbf{T}}^1 : \boldsymbol{\sigma}^0, \tag{68}$$

where $\boldsymbol{\varepsilon}^0$ and $\boldsymbol{\sigma}^0$ are the uniform strain and stress tensors when the material is homogeneous, and $\bar{\boldsymbol{\varepsilon}}^1$ and $\bar{\boldsymbol{\sigma}}^1$ are the volume average strain and stress tensors in a particle, respectively. Among various micromechanical schemes, the GSCM evaluates $\bar{\mathbf{E}}^1$ or $\bar{\mathbf{T}}^1$ based on the three-phase model where a particle is embedded in a finite matrix shell that, in turn, is embedded in an infinite equivalent medium with the yet-unknown effective properties of the composite, as shown in Fig. 4(a). It is noted that the matrix shell (region 2) in Fig. 4(a) corresponds to the interphase I in Fig. 1, and the equivalent homogeneous medium (region c) corresponds to the infinite matrix in Fig. 1. Because we have given the stress concentration tensor (Eq. (62)) for the inhomogeneity in the three-phase configuration, we can directly substitute it into Eq. (67) to calculate the effective compliance tensor of the composite. By doing so, it is found that the obtained effective bulk and shear moduli of the composite are identical to those given by Christensen and Lo (1979), and Huang et al. (1994). The effective shear modulus needs to be solved from a quadratic equation. Likewise, we can calculate the strain concentration tensor $\bar{\mathbf{E}}^1$ and substitute it into Eq. (66) to calculate the effective stiffness tensor, which is found to be

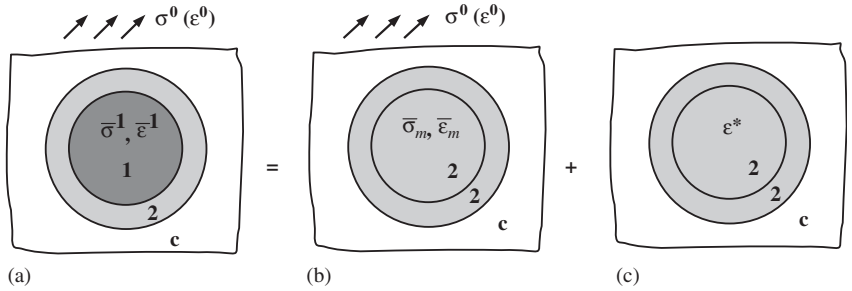

Fig. 4. The GSCM (three-phase) configuration for a composite containing spherical particles (a). The Eshelby equivalent inclusion method in a volume average sense for the three-phase configuration ((b) and (c)). Region 1 denotes a particle in the two-phase composite; region 2 represents the matrix; and region c denotes the equivalent homogeneous medium (composite).

identical to that obtained from Eq. (67). Thus, the results of the GSCM are confirmed in a unified tensorial approach.

In the following, instead of using the exact average stress concentration tensor in Eq. (62), we shall introduce the approximate volume average stress and strain concentration tensors by applying the Eshelby equivalent inclusion method to the three-phase configuration. To this end, we calculate the average stress concentration tensor by applying the equivalent inclusion method to the region 1, i.e. the spherical inhomogeneity, in Fig. 4(a). Assume that the volume average stress in this inhomogeneity in the three-phase configuration in Fig. 4(a) is $\bar{\boldsymbol{\sigma}}^1$ while the remote stress is $\boldsymbol{\sigma}^0$. For the same remote stress, when we replace the spherical inhomogeneity with the stiffness tensor $\mathbf{C}_1$ by the matrix material with the stiffness tensor $\mathbf{C}_2$, the volume average stress in the same region is denoted by $\bar{\boldsymbol{\sigma}}_m$, as shown in Fig. 4(b). This volume average stress $\bar{\boldsymbol{\sigma}}_m$ can be related to the remote stress by the relation

$$\bar{\boldsymbol{\sigma}}_m = \mathbf{B} : \boldsymbol{\sigma}^0, \tag{69}$$

where the fourth-order tensor $\mathbf{B}$ is equal to the classical stress concentration tensor $\mathbf{T}^0$. Generally, $\bar{\boldsymbol{\sigma}}_m$ is different from $\bar{\boldsymbol{\sigma}}^1$. As in the classical Eshelby equivalent inclusion method, the spherical matrix region 1 is further given a uniform eigenstrain $\boldsymbol{\varepsilon}^*$ (Fig. 4(c)) such that the following equivalency condition is satisfied:

$$\mathbf{C}_1 : (\bar{\boldsymbol{\varepsilon}}_m + \bar{\boldsymbol{\varepsilon}}') = \mathbf{C}_2 : (\bar{\boldsymbol{\varepsilon}}_m + \bar{\boldsymbol{\varepsilon}}' - \boldsymbol{\varepsilon}^*), \tag{70}$$

where $\bar{\boldsymbol{\varepsilon}}_m = \mathbf{D}_2 : \bar{\boldsymbol{\sigma}}_m = \mathbf{D}_2 : \mathbf{B} : \boldsymbol{\sigma}^0$. As in the work of Luo and Weng (1987), the disturbed strain $\bar{\boldsymbol{\varepsilon}}'$ is related to the interior Eshelby tensor $\bar{\mathbf{S}}^1$ through

$$\bar{\boldsymbol{\varepsilon}}' = \bar{\mathbf{S}}^1 : \boldsymbol{\varepsilon}^*, \tag{71}$$

where $\bar{\mathbf{S}}^1$ is given in Eq. (40). From the above relations, the volume average stress in the spherical particle can be obtained

$$\bar{\boldsymbol{\sigma}}^1 = \mathbf{C}_1 : \bar{\boldsymbol{\varepsilon}}^1 = \mathbf{C}_1 : (\bar{\boldsymbol{\varepsilon}}_m + \bar{\boldsymbol{\varepsilon}}') \equiv \bar{\mathbf{T}}^* : \boldsymbol{\sigma}^0, \tag{72}$$

where

$$\bar{\mathbf{T}}^* = [\mathbf{I}^{(4s)} - \mathbf{C}_1 : \bar{\mathbf{S}}^1 : (\mathbf{D}_1 - \mathbf{D}_2)]^{-1} : \mathbf{C}_1 : \mathbf{D}_2 : \mathbf{B} \equiv \alpha^* \mathbf{J} + \beta^* \mathbf{K}. \tag{73}$$

Likewise, the strain concentration tensor $\bar{\mathbf{E}}^*$, which relates the volume average strain $\bar{\boldsymbol{\varepsilon}}^1$ to the remote strain $\boldsymbol{\varepsilon}^0$ in the relation $\bar{\boldsymbol{\varepsilon}}^1 = \bar{\mathbf{E}}^* : \boldsymbol{\varepsilon}^0$, is given as

$$\bar{\mathbf{E}}^* = [\mathbf{I}^{(4s)} - \bar{\mathbf{S}}^1 : \mathbf{D}_2 : (\mathbf{C}_2 - \mathbf{C}_1)]^{-1} : \mathbf{A}, \tag{74}$$

where the fourth-order tensor $\mathbf{A}$ relates the volume average strain $\bar{\boldsymbol{\varepsilon}}_m$ to the remote strain $\boldsymbol{\varepsilon}^0$ through the relation $\bar{\boldsymbol{\varepsilon}}_m = \mathbf{A} : \boldsymbol{\varepsilon}^0$ (Fig. 4(b)), and $\mathbf{A} = \mathbf{D}_1 : \mathbf{B} : \mathbf{C}_2$.

It is found that the dilatational component α^* of the approximate average stress concentration tensor $\bar{\mathbf{T}}^*$ in Eq. (73) is identical to that of the exact average stress concentration tensor $\bar{\mathbf{T}}^1$. The expression of the deviatoric component β^* is different from that of the exact one. Fig. 5 shows the variations of the ratios β_1/β_0 and β^*/β_0 with the volume fraction of the inhomogeneities for two composites with different stiffness contrasts. β_0 is the deviatoric component of the classical stress concentration tensor for an inhomogeneity in an infinite medium. In calculating β_1 and β^* shown in Fig. 5, we need the effective elastic constants μ_c and v_c of the equivalent homogeneous medium (region c) in Fig. 4. These constants are calculated using the GSCM. It is seen that the values of β^* and β_1 are practically identical for these composites. The numerical results for other combinations of the stiffnesses of the three phases also exhibit the similar feature. Therefore, we can conclude that the approximate stress concentration tensor $\bar{\mathbf{T}}^*$ is very accurate. Thus, we shall replace $\bar{\mathbf{T}}^1$ in the general expression (67) with $\bar{\mathbf{T}}^*$ to predict the effective compliance tensor of composites containing randomly distributed spherical particles.

When substituting $\bar{\mathbf{T}}^*$ into Eq. (67), it is found that the obtained effective bulk modulus is identical to that given by the GSCM using $\bar{\mathbf{T}}^1$. Thus, it will not be discussed further. The effective shear modulus, denoted by μ_c, needs to be solved from the following quadratic equation in μ_* ($\mu_* = \mu_c/\mu_2$):

$$A\mu_*^2 + B\mu_* + C = 0, \tag{75}$$

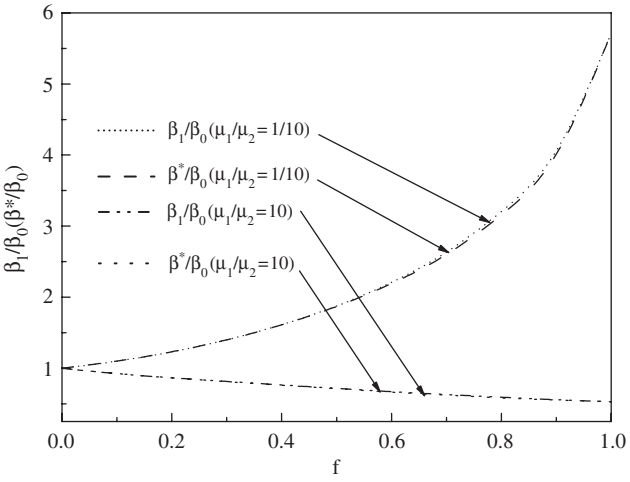

Fig. 5. Comparison of the deviatoric components (β_1 and β^*) of the exact volume average stress concentration tensor $\bar{\mathbf{T}}^1$ and the approximate $\bar{\mathbf{T}}^*$ obtained from the Eshelby equivalent inclusion method in the volume average sense ($v_1 = v_2 = 0.3$).

where

$$A = -[126f^{7/3} - 252f^{5/3} + 50(7 - 12\nu_2 + 8\nu_2^2)f](1 - g_{12}) + 4(7 - 10\nu_2)N,$$
$$B = [252f^{7/3} - 504f^{5/3} + 150(3 - \nu_2)\nu_2 f](1 - g_{12}) - 3(7 - 15\nu_2)N,$$
$$C = -[126f^{7/3} - 252f^{5/3} + 25(7 - \nu_2^2)f](1 - g_{12}) - (7 + 5\nu_2)N, \tag{76}$$

with $N = -7 + 5\nu_2 - 2g_{12}(4 - 5\nu_2)$ and $g_{12} = \mu_1/\mu_2$. It is seen that the coefficients A, B and C are much simpler than their counterparts in the classical GSCM. In the following, we shall compare the effective shear moduli given by the present model with those given by other methods for various composites to confirm its accuracy.

We first compare the effective shear moduli predicted by the present model with the classical Hashin–Shtrikman bounds (Hashin and Shtrikman, 1963), the GSCM (Christensen and Lo, 1979), the TOA (Torquato, 1998) and the numerical computations of Segurado and LLorca (2002) for three composites which contain stiff spheres with $\mu_1/\mu_2 = 10, \nu_1 = \nu_2 = 0.25$; $E_1 = 70\,\text{GPa}$, $\nu_1 = 0.2$, $E_2 = 3\,\text{GPa}$, $\nu_2 = 0.38$; and rigid spheres with $\nu_2 = 0.25$, respectively. The comparisons are shown in Figs. 6(a)–(c). In all the figures, μ_c denotes the effective shear modulus of the composite. It is seen that the effective shear modulus predicted by the present model is practically identical to those

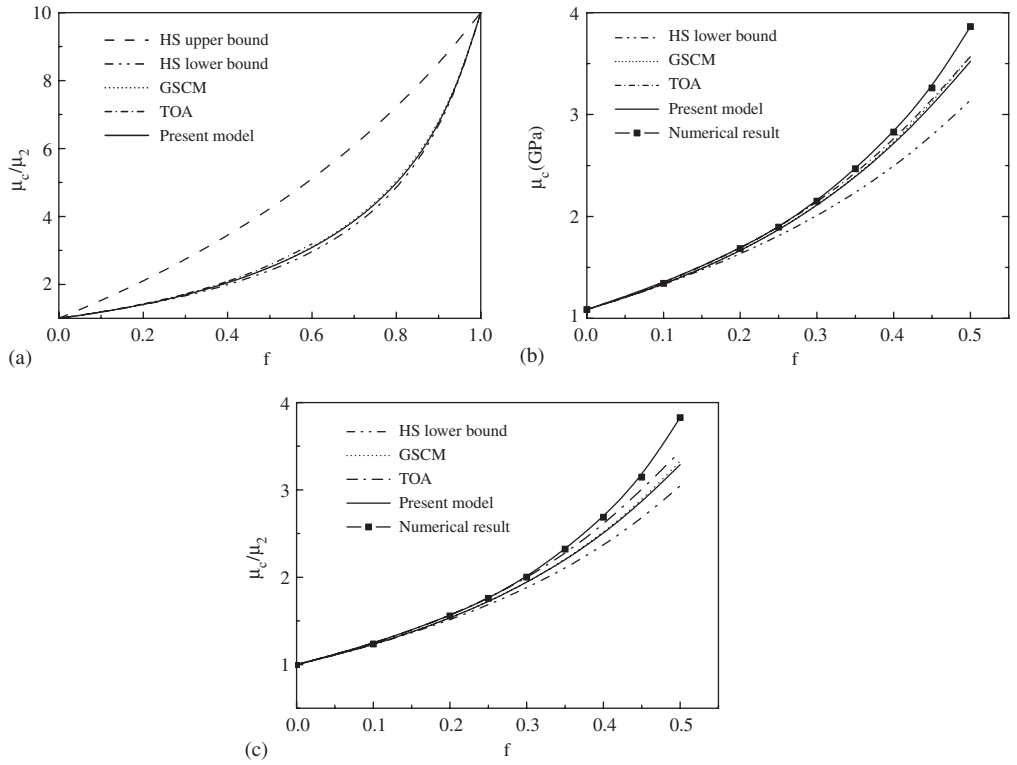

Fig. 6. Comparison of the effective shear moduli obtained from the present model with other methods for composites containing stiff spheres with $\mu_1/\mu_2 = 10, \nu_1 = \nu_2 = 0.25$ (a), glass beads $E_1 = 70\,\text{GPa}$, $\nu_1 = 0.2$, $E_2 = 3\,\text{GPa}$, $\nu_2 = 0.38$ (b), and rigid spheres with $\nu_2 = 0.25$ (c).

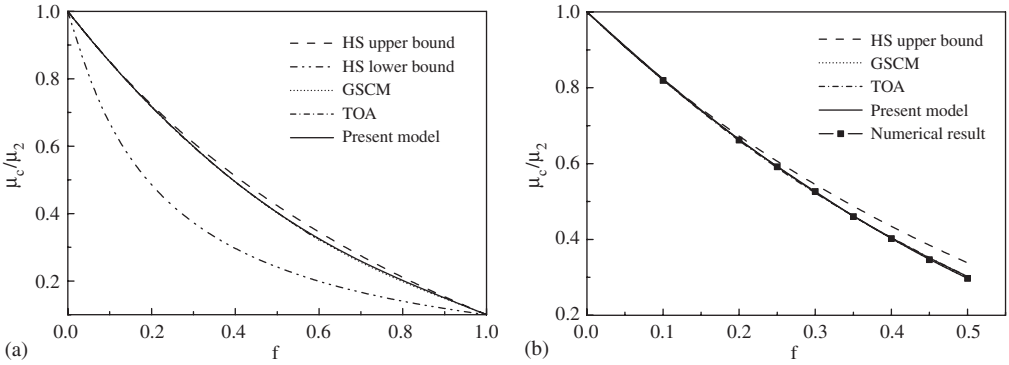

Fig. 7. Comparison of the effective shear moduli predicted by the present model with other methods for composites containing soft spheres with $\mu_1/\mu_2 = 1/10, \nu_1 = \nu_2 = 0.25$ (a), and voids with $\nu_2 = 0.25$ (b).

predicted by the GSCM and TOA for the composite with $\mu_1/\mu_2 = 10$ (Fig. 6(a)). For the other two composites, the present predictions are also almost indistinguishable from those of the GSCM (Figs. 6(b) and (c)). In Figs. 7(a) and (b), we compare the effective shear moduli predicted by the present model with other methods for two composites containing soft spheres and voids, respectively. It is seen that the present predictions are practically identical to those of the GSCM, the TOA and the numerical results (for composite containing voids). Moreover, it is found that the effective bulk and shear moduli obtained by substituting the strain concentration tensor in Eq. (74) into Eq. (66) are identical to those obtained by using $\tilde{\mathbf{T}}^*$ in Eq. (67). This feature demonstrates that the present model is also self-consistent.

8. Conclusions

The Eshelby and stress concentration tensors are derived for a spherical inhomogeneity with a graded shell embedded in an infinite elastic matrix. The general Eshelby tensors are then specialized to *inhomogeneous inclusions* in finite domains under fixed displacement or traction-free boundary conditions. These tensors are very useful for solving many problems in mechanics and materials science, e.g. the strain fields in core–shell nanoparticles which have a novel composite structure and myriad application in many fields. Finally, a micromechanical scheme is proposed to predict the effective moduli of composites containing spherical particles. The main advantage of this scheme is that, whilst its predictions of the effective moduli are almost identical to those of the classical generalized self-consistent method (GSCM) and the third-order approximation (TOA), the resulting expressions are simple and concise.

Acknowledgements

This work is supported by the National Natural Science Foundation of China under Grant nos. 10525209 and 10372004. The authors thank Professor J. LLorca and Dr J. Segurado for kindly providing their computational results. The authors also thank Professor B. L. Karihaloo of Cardiff University and Professor Gengkai Hu of Beijing Institute of Technology for helpful comments and discussions.

References

Abe, M., Suwa, T., 2004. Surface plasma resonance and magneto-optical enhancement in composites containing multicore-shell structured nanoparticles. Phys. Rev. B 70, 235103-1–235103-15.

Aboudi, J., 1991. Mechanics of Composite Materials—A Unified Micromechanical Approach. Elsevier, Amsterdam.

Benveniste, Y., 1987. A new approach to the application of Mori–Tanaka's theory in composite materials. Mech. Mater. 6, 147–157.

Bornert, M., Stolz, C., Zaoui, A., 1996. Morphologically representative pattern-based bounding in elasticity. J. Mech. Phys. Solids 44, 307–331.

Brongersma, M.L., 2003. Nanoshells: gifts in a gold wrapper. Nature Mater. 2, 296–297.

Christensen, R.M., Lo, K.H., 1979. Solutions for effective shear properties in three phase sphere and cylinder models. J. Mech. Phys. Solids 27, 315–330.

Dabbousi, B.O., Rodriguez-Viejo, J., Mikulec, F.V., Heine, J.R., Mattoussi, H., Ober, R., Jensen, K.F., Bawendi, M.G., 1997. (CdSe)ZnS core–shell quantum dots: synthesis and characterization of a size series of highly luminescent nanocrystallites. J. Phys. Chem. B 101, 9463–9475.

Danek, M., Jensen, K.F., Murray, C.B., Bawendi, M.G., 1996. Synthesis of luminescent thin-film CdSe/ZnSe quantum dot composites using CdSe quantum dots passivated with an overlayer of ZnSe. Chem. Mater. 8, 173–180.

Ding, K., Weng, G.J., 1998. The influence of moduli slope of a linearly graded matrix on the bulk moduli of some particle- and fiber-reinforced composites. J. Elasticity 53, 1–22.

Duan, H.L., Wang, J., Huang, Z.P., Luo, Z.Y., 2005. Stress concentration tensors of inhomogeneities with interface effects. Mech. Mater. 37, 723–736.

Eshelby, J.D., 1957. The determination of the elastic field of an ellipsoidal inclusion and related problems. Proc. R. Soc. Lond. A 241, 376–396.

Eshelby, J.D., 1959. The elastic field outside an ellipsoidal inclusion. Proc. R. Soc. Lond. A 252, 561–569.

Freund, L.B., Johnson, H.T., 2001. Influence of strain on functional characteristics of nanoelectronic devices. J. Mech. Phys. Solids 49, 1925–1935.

Goncharenko, A.V., 2004. Optical properties of core–shell particle composites. I. Linear response. Chem. Phys. Lett. 386, 25–31.

Gosling, T.J., Willis, J.R., 1995. Mechanical stability and electronic properties of buried strained quantum wire arrays. J. Appl. Phys. 77, 5601–5610.

Hashin, Z., Shtrikman, S.A., 1963. A variational approach to the theory of the elastic behavior of multiphase materials. J. Mech. Phys. Solids 11, 127–140.

He, L.X., Bester, G., Zunger, A., 2004. Strain-induced interfacial hole localization in self-assembled quantum dots: compressive InAs/GaAs versus tensile InAs/InSb. Phys. Rev. B 70, 235316-1–235316-9.

Herve, E., Zaoui, A., 1993. N-layered inclusion-based micromechanical modelling. Int. J. Eng. Sci. 31, 1–10.

Hill, R., 1963. Elastic properties of reinforced solids: some theoretical principles. J. Mech. Phys. Solids 11, 357–372.

Huang, Y., Hu, K.X., Wei, X., Chandra, A., 1994. A generalized self-consistent mechanics method for composite-materials with multiphase inclusions. J. Mech. Phys. Solids 42, 491–504.

Itskevich, I.E., Lyapin, S.G., Troyan, I.A., Klipstein, P.C., Eaves, L., Main, P.C., Henini, M., 1998. Energy levels in self-assembled InAs/GaAs quantum dots above the pressure-induced Gamma-X crossover. Phys. Rev. B 58, R4250–R4253.

Kim, H., Achermann, M., Balet, L.P., Hollingsworth, J.A., Klimov, V.I., 2005. Synthesis and characterization of Co/CdSe core–shell nanocomposites: bifunctional magnetic-optical nanocrystals. J. Am. Chem. Soc. 127, 544–546.

Lauhon, L.J., Gudiksen, M.S., Wang, D., Lieber, C.M., 2002. Epitaxial core–shell and core-multishell nanowire heterostructures. Nature 420, 57–61.

Li, S., Sauer, R., Wang, G., 2005. A circular inclusion in a finite domain I. The Dirichlet-Eshelby problem. Acta Mech. 179, 67–90.

Little, R.B., El-Sayed, M.A., Bryant, G.W., Burke, S., 2001. Formation of quantum-dot quantum-well heteronanostructures with large lattice mismatch: ZnS/CdS/ZnS. J. Chem. Phys. 114, 1813–1822.

Luo, H.A., Weng, G.J., 1987. On Eshelby's inclusion problem in a three-phase spherically concentric solid, and a modification of Mori–Tanaka's method. Mech. Mater. 6, 347–361.

Lutz, M.P., Zimmerman, R.W., 1996. Effect of the interphase zone on the bulk modulus of a particulate composite. J. Appl. Mech. 63, 855–861.

Ma, H.L., Hu, G.K., Huang, Z.P., 2004. A micromechanical method for particulate composites with finite particle concentration. Mech. Mater. 36, 359–368.

Milton, G.W., 2002. The Theory of Composites. Cambridge University Press, Cambridge.

Mori, T., Tanaka, K., 1973. Average stress in matrix and average elastic energy of materials with misfitting inclusions. Acta Metal. 21, 571–574.

Nemat-Nasser, S., Hori, M., 1999. Micromechanics: Overall Properties of Heterogeneous Materials, second ed. Elsevier, Amsterdam.

Ostoja-Starzewski, M., Jasiuk, I., Wang, W., Alzebdeh, K., 1996. Composites with functionally graded interfaces: meso-continuum concept and effective transverse conductivity. Acta Mater. 44, 2057–2066.

Peng, X.G., Schlamp, M.C., Kadavanich, A.V., Alivisatos, A.P., 1997. Epitaxial growth of highly luminescent CdSe/CdS core/shell nanocrystals with photostability and electronic accessibility. J. Am. Chem. Soc. 119, 7019–7029.

Perez-Conde, J., Bhattacharjee, A.K., 2003. Electronic structure and optical properties of ZnS/CdS nanoheterostructures. Phys. Rev. B 67, 235303-1–235303-4.

Ponte Castañeda, P., Suquet, P., 1998. Nonlinear composites. Adv. Appl. Mech. 34, 171–302.

Rockenberger, J., Troger, L., Rogach, A.L., Tischer, M., Grundmann, M., Eychmuller, A., Weller, H., 1998. The contribution of particle core and surface to strain, disorder and vibrations in thiolcapped CdTe nanocrystals. J. Chem. Phys. 108, 7807–7815.

Segurado, J., LLorca, J., 2002. A numerical approximation to the elastic properties of sphere-reinforced composites. J. Mech. Phys. Solids 50, 2107–2121.

Talbot, D.R.S., Willis, J.R., 1985. Variational principles for inhomogeneous nonlinear media. IMA J. Appl. Math. 35, 39–54.

Theocaris, P.S., 1987. The Mesophase Concept in Composites. Springer, Berlin.

Torquato, S., 1998. Effective stiffness tensor of composite media: II. Applications to isotropic dispersions. J. Mech. Phys. Solids 46, 1411–1440.

Torquato, S., 2002. Random Heterogeneous Materials: Microstructure and Macroscopic Properties. Springer, New York.

Tzika, P.A., Boyce, M.C., Parks, D.M., 2000. Micromechanics of deformation in particle-toughened polyamides. J. Mech. Phys. Solids 48, 1893–1929.

Walpole, L.J., 1981. Elastic behaviour of composite materials: theoretical foundations. Adv. Appl. Mech. 21, 169–242.

Wang, W., Jasiuk, I., 1998. Effective elastic constants of particulate composites with inhomogeneous interphases. J. Compos. Mater. 32, 1391–1424.

Wang, G., Li, S., Sauer, R., 2005. A circular inclusion in a finite domain II. The Neumann-Eshelby problem. Acta Mech. 179, 91–110.

Weng, G.J., 2003. Effective bulk moduli of two functionally graded composites. Acta Mech. 166, 57–67.

Williamson, A.J., Zunger, A., 1999. InAs quantum dots: predicted electronic structure of free-standing versus GaAs-embedded structures. Phys. Rev. B 59, 15819–15824.

Willis, J.R., 2000. The overall response of nonlinear composite media. Eur. J. Mech. A/Solids 19, S165–S184.

Wylie, C.R., Barrett, L.C., 1982. Advanced Engineering Mathematics, second ed. McGraw-Hill, New York.

Zheng, Q.S., Du, D.X., 2001. An explicit and universally applicable estimate for the effective properties of multiphase composites which accounts for inclusion distribution. J. Mech. Phys. Solids 49, 2765–2788.

Zhou, H.S., Honma, I., Haus, J.W., Sasabe, H., Komiyama, H., 1996. Synthesis and optical properties of coated nanoparticle composites. J. Luminescence 70, 21–34.